Biomaterials 95 (2016) 11–21

Contents lists available at ScienceDirect

Biomaterials

journal homepage: www.elsevier.com/locate/biomaterials

Nanodiamond modified copolymer scaffolds affects tumour progression of early neoplastic oral keratinocytes

Salwa Suliman [a, b, c, **], Kamal Mustafa [a], Anke Krueger [d], Doris Steinmüller-Nethl [e], Anna Finne-Wistrand [f], Tereza Osdal [g], Amani O. Hamza [b], Yang Sun [a, f], Himalaya Parajuli [b, c], Thilo Waag [d], Joachim Nickel [h, i], Anne Christine Johannessen [b, j, k], Emmet McCormack [g, l], Daniela Elena Costea [b, c, j, k, *]

[a] Department of Clinical Dentistry, Center for Clinical Dental Research, University of Bergen, Norway
[b] Gade Laboratory for Pathology, Department of Clinical Medicine, University of Bergen, Bergen, Norway
[c] Center for International Health, Department of Global Public Health and Primary Care, University of Bergen, Bergen, Norway
[d] Institute of Organic Chemistry, University of Würzburg, Würzburg, Germany
[e] DiaCoating GmbH, Innsbruck, Austria
[f] Department of Fibre and Polymer Technology, KTH, Royal Institute of Technology, Stockholm, Sweden
[g] Department of Clinical Science, Hematology Section, University of Bergen, Bergen, Norway
[h] Chair Tissue Engineering and Regenerative Medicine, University Hospital Würzburg, Germany
[i] Fraunhofer Institute for Interfacial Engineering and Biotechnology IGB, Translational Center 'Regenerative Therapies for Oncology and Musculoskeletal Diseases'– Würzburg Branch, Germany
[j] Department of Pathology, Haukeland University Hospital, Bergen, Norway
[k] Centre for Cancer Biomarkers, Department of Clinical Medicine, University of Bergen, Bergen, Norway
[l] Department of Medicine, Haematology Section, Haukeland University Hospital, Bergen, Norway

ARTICLE INFO

Article history:
Received 29 March 2016
Accepted 3 April 2016
Available online 6 April 2016

Keywords:
Bone tissue engineering
Biocompatibility
Tumorigenicity
Microenvironment
Oral squamous cell carcinoma
BMP-2

ABSTRACT

This study aimed to evaluate the tumorigenic potential of functionalising poly(LLA-co-CL) scaffolds. The copolymer scaffolds were functionalised with nanodiamonds (nDP) or with nDP and physisorbed BMP-2 (nDP-PHY) to enhance osteoinductivity. Culturing early neoplastic dysplastic keratinocytes (DOK^{Luc}) on nDP modified scaffolds reduced significantly their subsequent sphere formation ability and decreased significantly the cells' proliferation in the supra-basal layers of *in vitro* 3D oral neoplastic mucosa (3D-OT) when compared to DOK^{Luc} previously cultured on nDP-PHY scaffolds. Using an *in vivo* non-invasive environmentally-induced oral carcinogenesis model, nDP scaffolds were observed to reduce bioluminescence intensity of tumours formed by DOK^{Luc} + carcinoma associated fibroblasts (CAF). nDP modification was also found to promote differentiation of DOK^{Luc} both *in vitro* in 3D-OT and *in vivo* in xenografts formed by DOK^{Luc} alone. The nDP-PHY scaffold had the highest number of invasive tumours formed by DOK^{Luc} + CAF outside the scaffold area compared to the nDP and control scaffolds. In conclusion, *in vitro* and *in vivo* results presented here demonstrate that nDP modified copolymer scaffolds are able to decrease the tumorigenic potential of DOK^{Luc}, while confirming concerns for the therapeutic use of BMP-2 for reconstruction of bone defects in oral cancer patients due to its tumour promoting capabilities.

1. Introduction

Extensive efforts have been made in bone tissue engineering (BTE) to combine osteogenic growth factors with scaffolds in order to control their release, thus regenerating bone defects with minimal side effects [1]. Bone morphogenetic proteins (BMPs) are members of the large TGF-β superfamily, which play a crucial role in regulating cell proliferation, apoptosis, differentiation and

* Corresponding author. Gade Laboratory for Pathology, Department of Clinical Medicine, Haukeland University Hospital, University of Bergen, N-5021, Bergen, Norway.
** Corresponding author. Gade Laboratory for Pathology, Department of Clinical Medicine, Haukeland University Hospital, University of Bergen, N-5021, Bergen, Norway.
E-mail addresses: salwa.suliman@uib.no (S. Suliman), daniela.costea@uib.no (D.E. Costea).

http://dx.doi.org/10.1016/j.biomaterials.2016.04.002
0142-9612/

organogenesis [2]. Clinical trials using large amounts of BMP-2 in an absorbable collagen sponge were carried out in several orthopaedic approaches. These ranged from spinal fusions to long bone fractures and more recently augmenting the alveolar ridge, cleft reconstructions and sinus lift surgeries [3–5]. The use of BMP-2 was reported advantageous over the 'gold standard', autologous bone graft, by shortening the operating time and decreasing hospitalisation costs. However, its off-label use even in oral and maxillofacial surgeries came with several side effects [6–8]. Those side effects were attributed to uncontrolled release of high doses of the embedded growth factor. Cancer has been an alarming adverse effect reported by studies on spinal surgeries using BMP-2, while some studies showed a link between use of BMP-2 and carcinogenesis; others did not find this association [9,10]. Nevertheless, the observed increase in cancer incidence, while low and uncertain, remains a real concern for the use of recombinant BMP-2 (rhBMP-2). In addition, several studies expressed concern and had implications for the safe delivery of BMP-2 when reconstructing bone defects after extensive surgeries for treating oral squamous cell carcinomas (OSCC) [11,12]. *In vitro* and *in vivo* investigations of the effects of BMP-2 on OSCC cells showed an increase in the invasive potential and poor survival rate after exposure to BMP-2 [11,12]. Moreover, this association was also observed for gastric and breast cancer cells [13]. The association between BMP-2 and OSCC was also indicated from patient studies. In a cohort of 149 patients with oral, head and neck squamous cell carcinoma analysed retrospectively; tumours with higher BMP-2 expression were found to have higher rates of local failure and local recurrence [14]. In normal human keratinocytes *in vitro*, BMP-2 was shown to modulate the expression of molecules related to Wnt signalling which may be affected by the fate of keratinocytes, such as their proliferation, migration and differentiation [15]. Also, epithelial to mesenchymal transition in human skin would healing was shown to be modulated by BMP-2 in human normal keratinocytes *in vitro* [16].

Nanodiamond (nDP), a carbon derived nanoparticle of about 4–5 nm in diameter with low chemical reactivity and unique physical properties [17,18] have emerged as potentially useful materials in bone regeneration. As a stable colloid, they were used to deliver osteogenic molecules such as BMP-2 for promoting bone formation [19]. Cell viability assays showed that nDP are not toxic to a variety of cell types [20]. They have been tested for their cytotoxicity in suspensions and it was reported that higher concentrations affect cell proliferation and metabolic activities in macrophages [21]. Nano-sized materials demonstrated controversial results during long term implantations in murine models [22], but assessment of carcinogenicity of nDP is an unexplored area, especially in the context of biomaterial modifications.

Aliphatic polymers have been commonly used in the biomedical field and also approved by the Food and Drug Administration in several clinical products [23]. Copolymer scaffolds synthesised from L-lactide (LLA) and ε-caprolactone (ε-CL), (poly[LLA-co-CL]), have been comprehensively validated as BTE scaffolds with encouraging cyto-compatibility and osteoconductivtiy outcomes both *in vitro* and *in vivo* [24–26]. Modifying these copolymer scaffolds with nDP improved their mechanical properties and enhanced their wettability which positively affected their osteoconductive potential [27,28]. A modality of delivering BMP-2 to bone defects using poly(LLA-co-CL) scaffolds modified with nDP was recently developed in an attempt to reduce side effects from conventional high dose burst delivery. It proved successful physisorption of BMP-2 onto the nDP; sustained low amounts of bioactive BMP-2 released up to 70 days, and enhanced osteogenic differentiation of human mesenchymal stem cells, in addition to accelerated bone formation in a rat mandible critical-sized defect [29]. This construct carries two stimulating factors, nanodiamond particles and BMP-2, which makes a testing of its biocompatibility on one hand side and long term adverse effects on the other hand crucial. Biomaterials implanted, such as those for the purpose of tissue regeneration have been reported on their potential of inducing foreign body carcinogenesis and are usually tested in long term 2 year rodent assays or half a year in transgenic mice [30]. Although this phenomenon is rarely encountered in humans [31], it cannot be overlooked and every new biomaterial is required to rigorously undergo adverse effect testing for regulatory reasons [32].

An *in vivo* environmentally-induced oral carcinogenesis model to screen the tumorigenic potential of BTE scaffolds has been recently reported by our research group to successfully and reliably monitor the scaffolds by bioluminescence (BLI) in an attempt to surpass the limitations of the long term rodent assays [33]. The model has been developed using early neoplastic dysplastic oral keratinocytes (DOK) and the poly(LLA-co-CL) scaffolds. The DOK are derived from a tongue dysplasia (premalignant oral mucosa lesion) that progressed after 11 years into a well-differentiated OSCC [34]. They were reported to be partly transformed but non-tumorigenic in NUDE mice and our previous research on non-obese diabetic/severe combined immunodeficient (NOD/SCID) mice showed that DOK at a low density were tumorigenic only when co-inoculated with carcinoma associated fibroblasts (CAF) [35]. The use of dysplastic cells instead of normal keratinocytes was carried to gain advantage over the time spent to reproduce mutagenic events in tumour models with experimental setting from normal cells [36]. We therefore chose to use the early neoplastic cells, DOK, as a screening tool to evaluate the tumour promoting potential of scaffolds, providing a faster alternative to the long 'lifetime' *in vivo* models [33].

In this current investigation the developed model was used along with several *in vitro* functional tumorigenicity assays to evaluate the effect of functionalising poly(LLA-co-CL) scaffolds with nDP or with nDP and physisorbed BMP-2.

The authors postulate that the functionalised poly(LLA-co-CL) scaffolds with nDP will have an effect on the differentiation of DOK owing to nDP's inherent functional groups that were shown to enhance the differentiation of other type of cells [28].

2. Materials and methods

2.1. Scaffold fabrication and modification with nDP and nDP + BMP-2

Poly(LLA-co-CL) was synthesised from 75 mol % L-lactide and 25 mol % ε-caprolactone as previously described [26,37] confirmed by proton nuclear magnetic resonance (Bruker Avance 400, Billerica, MA, USA). The purified copolymer had a number average molecular weight of ≈100,000 Da and a molar mass dispersity ≈1.3 determined by size exclusion chromatography (Polymer Laboratories, U.K.). The porous poly(LLA-co-CL) scaffolds were prepared by solvent casting particulate leaching and a disc-shaped scaffold (diameter ≈ 12 mm/thickness ≈ 1.3 mm) for *in vitro* experiments and (diameter ≈ 6 mm/thickness ≈ 1.3 mm) for *in vivo* experiments [26]. Porosity was >83% measured by micro computed tomography, (Skyscan 1172, Bruker) (40 kV and 2.4 μm voxel).

Detonation diamond purified by acid (Gansu Lingyun Corp., Lanzhou, China) was milled for dispersion using a method previously described [38] producing a narrow size distribution at ~5 nm particle diameter (measured by dynamic light scattering in water) and low agglomeration of the diamond particles. Briefly, scaffolds were modified with the nDP solution (2 wt %, i.e. 20 mg/ml) by a vacuum technique: 0.5 ml nDP solution and one scaffold were put in a glass beaker and perfused in vacuum (Oerlikon Leybold, TRIVAC

D 65B) as previously described [29].

Recombinant BMP-2 expressed in *Escherichia coli* (*E-coli*), isolated from inclusion bodies, renatured and purified and the poly(LLA-co-CL) scaffolds were modified using the nanodiamond particles and physisorbed with BMP-2 as previously described [29]. Each scaffold contained 1 μg of BMP-2.

Unmodified poly(LLA-co-CL) scaffolds are denoted by CL scaffold, scaffolds modified with nanodiamond by nDP scaffold and scaffolds modified with nanodiamond plus physisorbed with BMP-2 by nDP-PHY scaffold.

2.2. Cell source and maintenance

Three different cell types were used in the *in vitro* and/or *in vivo* experiments.

2.2.1. Early neoplastic dysplastic oral keratinocyte (DOK)

DOK cell line purchased from The European Collection of Cell Cultures (Salisbury, Wiltshire, UK) [34] was transduced to contain the firefly luciferase as described previously [33]. Briefly, infectious retroviral vector particles were produced in Phoenix A cells (LGC Standards AB, Boras, Sweden). Transduction with a luciferase expressing construct, L192, coding for the luciferase enzyme and co-transduced with the tetracycline-regulated transactivator (tTA) was carried out as previously described [39]. Cells were selected with puromycin (1 μg/ml) (Sigma, St Louis, MO, USA). Transduced DOK were designated as DOK^{Luc}. They were maintained in Dulbecco's Modified Eagle's Medium (DMEM) supplemented with 10% Foetal Calf Serum (FCS, Invitrogen, Waltham, MA, USA), 20 μg/ml L-glutamine, 5 μg/ml hydrocortisone (Sigma).

2.2.2. Carcinoma associated fibroblasts (CAF)

CAF were isolated from histologically confirmed OSCC, after informed consent using a previously described explant technique [40] and were cultured in FAD medium: DMEM/Ham's F12 1:3 mixture, 1% L-glutamine, 0.4 μg/ml hydrocortisone, 50 μg/ml ascorbic acid, 10 ng/ml EGF, 5 μg/ml insulin and 20 μg/ml transferrin and linoleic acid (all from Sigma) with 10% FCS.

2.2.3. Gingival fibroblasts (GF)

GF were isolated from normal human oral mucosa of individuals undergoing third molar extraction after informed consent, using the aforementioned explant technique and maintained in DMEM high glucose + 10% FCS (Sigma).

2.3. In vitro functional assays for tumorigenic properties

The CL, nDP and nDP-PHY scaffolds (n = 20 per scaffold type) were placed in 48-well plates. DOK^{Luc} (25×10^4 per scaffold) were seeded on top and allowed to culture. After 1 week the DOK^{Luc} were trypsinised from the scaffolds and allowed to plate and propagate for 19 days in tissue culture flasks (Nunc, ThermoScientific, Wilmington, Delaware, USA) to obtain sufficient number of cells before exposing them to the following functional assays.

2.3.1. Sphere formation assay

To obtain non-adherent surfaces 48-well tissue culture plates were coated overnight with 1 ml of 12 mg/ml stock of 2-hydroxyethyl methacrylate (Sigma) in 95% methanol. Five hundred DOK^{Luc} were mixed in 475 μl of FAD medium with 25 μl of Matrigel (BD Biosciences, NJ, USA). The cells were allowed to grow for 3 weeks before images (n = 6 per well) were obtained of each well and spheres larger than 40 μm in diameter were counted, considered to include spheres formed of more than 50 cells approximately.

2.3.2. Three-dimensional organotypic cultures (3D-OT)

GF or CAF were used at early passages (less than 10) to create the stromal compartment of the 3D-OT. The collagen matrix was prepared on ice by mixing 7 vol of rat tail collagen type I (BD bioscience), 2 vol of reconstitution buffer (composed of 2.2 g $NaHCO_3$, 0.6 g NaOH, 4.766 g HEPES (all from Sigma) in 100 ml dH_2O) to achieve a pH of 7.2 and 1 vol of DMEM 4× (Sigma). Each type of fibroblast was first re-suspended in 1 vol of FCS in a final concentration of 2.5×10^5 cells/matrix and then added to the aforementioned mixture. Seven hundred μl of this mixture was added onto each well of 24 well dishes (Nunc, Thermo Fisher Scientific, Waltham, MA, USA). After 20 min incubation at 37 °C, the matrix solidified and 1 ml of routine medium for the respective fibroblast type was added on top. One day later, DOK^{Luc} extracted from the scaffolds were re-suspended in DOK medium and seeded on top of the collagen biomatrix at a concentration of 5×10^5 cells per matrix to re-construct the epithelial compartment of the 3D-OT. After 2 days of co-culture, the 3D-OTs were detached and lifted on a stainless metal grid to keep them at the air liquid interface for a week in the OT medium. Two thirds of the medium was changed every 2nd day. The OT medium was composed of DMEM:Ham-F12 1:3 mixture, supplemented with 0.4 μg/ml hydrocortisone, 20 μg/ml transferrin, 50 μg/ml L-ascorbic acid, 1 mg/ml linoleic acid-albumin, 20 μg/ml L-Glutamine (all from Sigma), 5 μg/ml insulin (Novo Nordisk, Bagsværd, Denmark). After 10 days of co-culture the 3D-OT were harvested and fixed in 4% paraformaldehyde (PFA) before processing for paraffin embedding. As a positive control, DOK^{Luc} routinely grown in tissue culture plates were harvested and cultured on top of collagen biomatrix with CAF instead of GF, and following the same aforementioned procedure. This was inspired from our previous research which showed that the invasion of malignant oral keratinocytes was significantly greater when CAF were embedded in the biomatrix compared to when normal oral fibroblasts were used [35].

2.4. Animal procedures

The different scaffolds were also evaluated for the tumorigenic potential *in vivo* using our recently developed microenvironmentally-induced model employing BLI to monitor the tumour formation non-invasively. NOD-*scid* $IL2r\gamma^{null}$ (NSG) female mice (University of Bergen, Bergen, Norway) were used at 8–10 weeks old.

The scaffolds were first pre-wet with DOK medium before being seeded with cells, DOK^{Luc} alone or DOK^{Luc} + CAFs (positive control). Seeding density was 1×10^4 and 1×10^5 for DOK^{Luc} and CAF respectively. Plates were vortexed and cells allowed to attach overnight. Subcutaneous operating procedure was performed as previously described under Isoflurane gas anaesthesia, and all efforts were made to minimise suffering [41]. Two scaffolds were implanted into the back of each mouse, one scaffold with DOK^{Luc} alone and the other with DOK^{Luc} + CAF.

Optical BLI: To non-invasively monitor tumour formation *in vivo*, mice were depilated and scanned following intraperitoneal delivery of 150 mg/kg of D-luciferin (Biosynth, AG, Staad Switzerland). Images were captured using In Vivo MS FX PRO (Carestream Health Inc. Rochester, NY) and analysed using Carestream MI SE version 5.0.6.20, 1 exposure of 90 s duration. At 14 weeks animals were euthanized (n = 6 per scaffold type). Xenografts were carefully dissected from the subcutaneous region and fixed in 4% PFA before being processed for paraffin embedding.

2.5. Immunohistochemistry

Paraffin embedded 3D-OTs and tumour xenografts were sectioned at 3–4 μm and stained with hematoxylin-eosin (H&E) (Sigma). Sectioned 3D-OTs were additionally stained for Ki67

(Dako, A/S, Glostrup, Denmark) to evaluate proliferating DOK^{Luc}, EGFR (Dako) and Involucrin (NovoCastra, Wetzlar, Germany) to evaluate the degree of differentiation and E-Cadherin (Dako) to evaluate the tissue coherence. The primary antibodies (Ab) and titrations used were as follows: mouse monoclonal antibody (mAb) Ki-67 clone MIB-1 1:25; mAb EGFR clone H11 1:50; mAb Involucrin 1:500 and mAb E-cadherin clone NCH-38 1:3000. All Ab were diluted in antibody diluent (Dako). Sections were then counter-stained with hematoxylin (DAKO), dehydrated and cover-slipped. The bound reaction was visualized using 3, 3′-diaminobenzidine tetra hydrochloride (DAB, Dako). Sections of tonsils and normal oral mucosa served as positive controls. For negative controls, sections incubated with antibody diluent only were used.

2.6. Quantification of staining

The depth of invasion in the 3D-OTs was evaluated on H&E sections using a light microscope and the software Olympus DP.Soft 5.0. The central and the two outer 5ths of 3D-OTs were excluded due to technical variations. The depth of invasion was determined every 100 μm as the vertical distance from an arbitrary line drawn through the upper remnants of the collagen biomatrix and representing the basement membrane till the deepest limit of invading DOK^{Luc} in the respective field. At least 6 measurements were taken per tissue.

Immunostained sections were imaged using a Nikon Eclipse 80i microscope equipped with a Nikon DS-Fi1 camera (Tokyo, Japan), to quantify positively stained Ki67, involucrin, EGFR and E-cadherin cells. Ki-67 positively stained nuclei were counted separately in the basal and para-basal area and in the supra-basal area for each sample and presented as a percentage of the total number of nuclei in the epithelial compartment. The open source digital image analysis software ImageJ (v.1.46r) (National Institute of Health, USA) was used to count positively stained Ki67 nuclei. Recently developed Plugin IHC Profiler compatible with ImageJ was used for quantifying involucrin, EGFR and E-cadherin stain. An area of interest was drawn around the (basal and para-basal area) and another area of interest around the supra-basal area and each was quantified separately. The software creates a pixel-by-pixel analysis profile of a digital immunohistochemistry image and further scoring it using a four level system [42]. The highly positive scores were used for each area and a ratio of supra-basal area to basal and para-basal areas was calculated to plot quantification graphs.

2.7. Ethical approval

The ethical approvals for sample collection from OSCC patients and individuals undergoing third molar extraction samples were obtained from the Regional Committee for Medical and Health Research Ethics (REK # 2010/481). Samples were collected following informed consent of the patients.

Animal experiments were approved by the Norwegian Animal Research Authority and conducted in strict accordance with the European Convention for the Protection of Vertebrates used for Scientific Purposes (FOTS no. 20135297).

2.8. Statistical analysis

All data are presented as the mean values ± standard error of the mean (SEM). Significant difference in the sphere formation, depth of invasion between groups in 3D-OT and significant difference in immunohistochemical stain quantification was tested by One-way ANOVA, followed by a multiple comparison Tukey test. Paired *t*-test was used to compare differences between the total photon counts of the different tumours (DOK^{Luc} or DOK^{Luc} + CAF) in each scaffold group. SPSS ver. 21/22 (IBM, NY, USA) was used and the level of significance was set to $p < 0.05$.

3. Results

3.1. DOK^{Luc} cells previously cultured on nDP scaffolds showed decreased sphere formation ability when compared to DOK^{Luc} previously cultured on other scaffolds

When retrieved after being seeded on different scaffolds for 1 week and further propagated in culture on adherent plates, DOK^{Luc} cells displayed a typical epithelial morphology for all conditions. There was no difference in the proliferation rate of cells seeded on the different scaffolds, but DOK^{Luc} previously seeded on nDP scaffolds contained a number of cells with a larger cell surface area when compared with cells seeded on other scaffolds (Fig. 1A, yellow arrows). The DOK^{Luc} extracted from the different scaffolds were also subjected to non-adherent culture to evaluate their anchorage independent growth and hence their tumorigenic potential. After being cultured on nDP coated scaffolds, DOK^{Luc} formed a significantly reduced number of spheres compared with the CL and nDP-PHY scaffolds (Fig. 1 B, C).

3.2. DOK^{Luc} previously grown on nDP scaffolds displayed a less abnormal proliferation pattern and increased differentiating capacities in 3D-OT models when compared with DOK^{Luc} previously grown on other scaffolds

The DOK^{Luc} cells grown on nDP-PHY scaffolds and the positive control (DOK^{Luc} grown on CAF) showed the highest percentage of Ki67 positive nuclei in the (basal and para-basal) layers, which was significantly higher for nDP-PHY modified scaffolds when compared to the other scaffold types (Fig. 2 A). The cells from the nDP-PHY modified scaffolds ($p = 0.011$) and the positive control ($p = 0.007$) had significantly increased expression of Ki-67 in the supra-basal layers, compared with cells from nDP modified scaffolds. The cells from the nDP and CL scaffolds showed cell proliferation confined mainly to the basal layer.

Assessment of the epithelial differentiation marker involucrin showed in the positive controls for stimulating the tumorigenesis (DOK^{Luc} on CAFs 3D-OT) a random expression throughout all epithelial layers, without the normal polarisation of stronger expression in the superficial layers and weaker expression in the basal/para-basal layers as found in a normal oral epithelium. The models constructed with DOK^{Luc} from the scaffolds showed also involucrin expression in all epithelial layers but DOK^{Luc} previously grown on nDP-PHY scaffolds showed a significantly reduced expression of involucrin in the supra-basal layers and mostly in the para-basal layers. This indicated an abnormal pattern of differentiation, similar to the positive control for tumorigenesis. On the contrary, involucrin was significantly highly expressed in the upper (supra-basal) epithelial layers of the 3D-OT formed by DOK^{Luc} from nDP scaffolds (Fig. 2 B), a pattern of expression closest to that found in normal human oral mucosa. The pattern of EGFR staining in our 3D-OTs was also investigated and an opposite trend to the involucrin staining was observed in all conditions, including the positive control. However, the difference between groups was not statistically significant.

3.3. DOK^{Luc} cells previously grown on nDP scaffolds displayed lower invasive potential and increased expression of cell adhesion molecule E-cadherin when compared to DOK^{Luc} previously grown on other scaffolds

DOK^{Luc} showed the highest invasive potential (deeper invasion) when cultured on the positive control (with CAFs in the biomatrix).

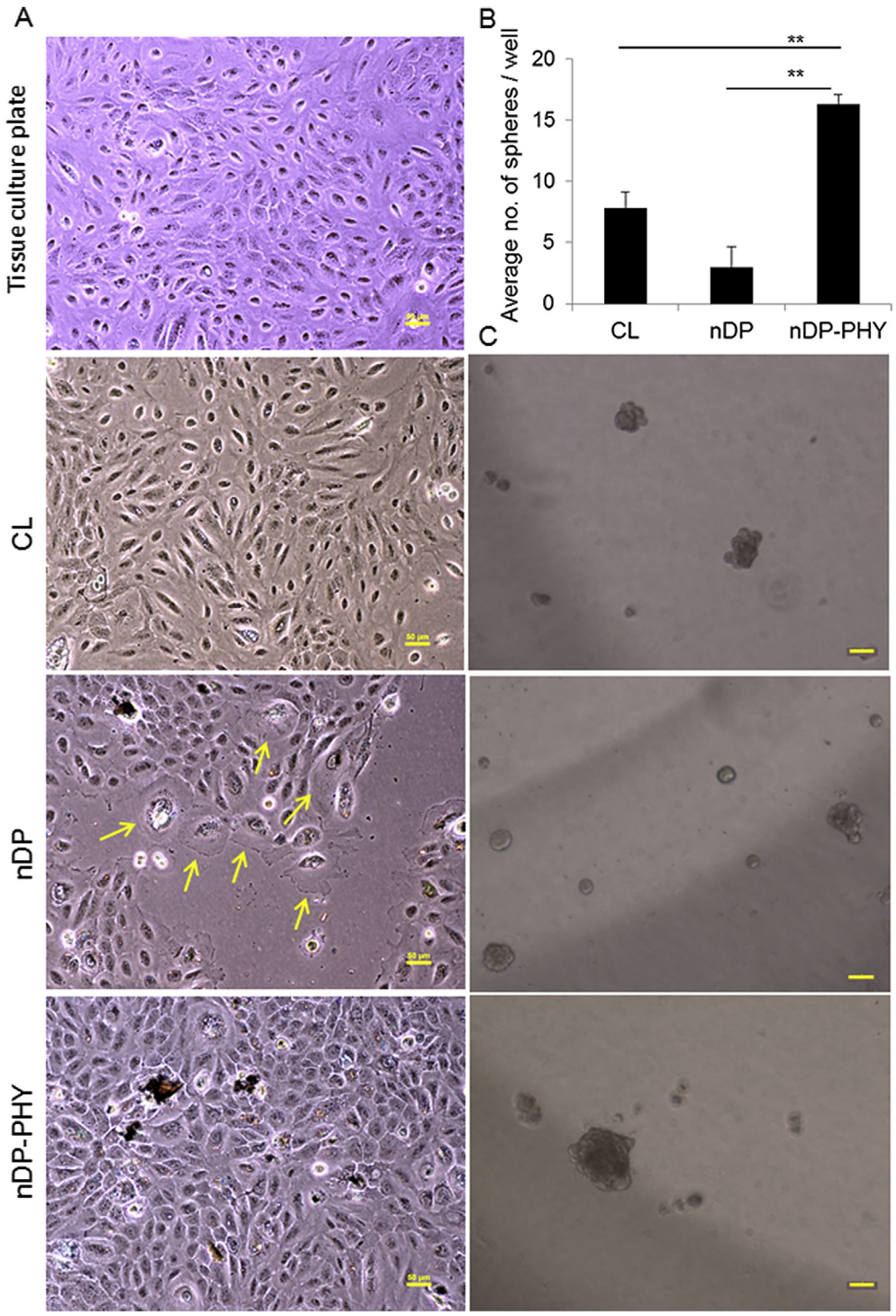

Fig. 1. Morphology and adherence-independent growth behaviour of DOK^{Luc} after being cultured on the different scaffolds. (A) Light micrograph of the DOK^{Luc} cultured in a tissue culture plate and representative micrographs of DOK^{Luc} propagated 1 week after being extracted from the different scaffolds. The cells preserved their epithelial morphology in all conditions. A number of cells previously grown on nDP scaffold displayed abundant cytoplasm and larger surface areas (yellow arrows). **(B)** Average number of spheres (larger than 40 μm in diameter) formed after 21 days in culture. **(C)** Representative light micrographs showing spheres formed by DOK^{Luc} extracted from different scaffolds. Scale bar 50 μm. Error bars represent SEM. *$p < 0.05$, **<0.01. (For interpretation of the references to colour in this figure legend, the reader is referred to the web version of this article.)

This invasive potential was similar to that of DOK^{Luc} previously seeded on nDP-PHY scaffolds but cultured on normal GF in 3D-OT (Fig. 3B). A significant decrease in DOK^{Luc} invasion was observed in the 3D-OTs that were seeded with DOK^{Luc} from nDP scaffold (Fig. 3B). The DOK^{Luc} grown on collagen biomatrices populated with CAF showed an expansion of intercellular spaces along the length of the epithelium. Further investigation of the cell adhesion molecule E-cadherin was done in this study, promoted by the increased spongiosis and invasion previously mentioned to occur in the epithelium of 3D-OTs, particularly in the positive control group. E-cadherin showed an expression generally confined to the cell membranes of epithelium formed from DOK^{Luc} in all groups, but

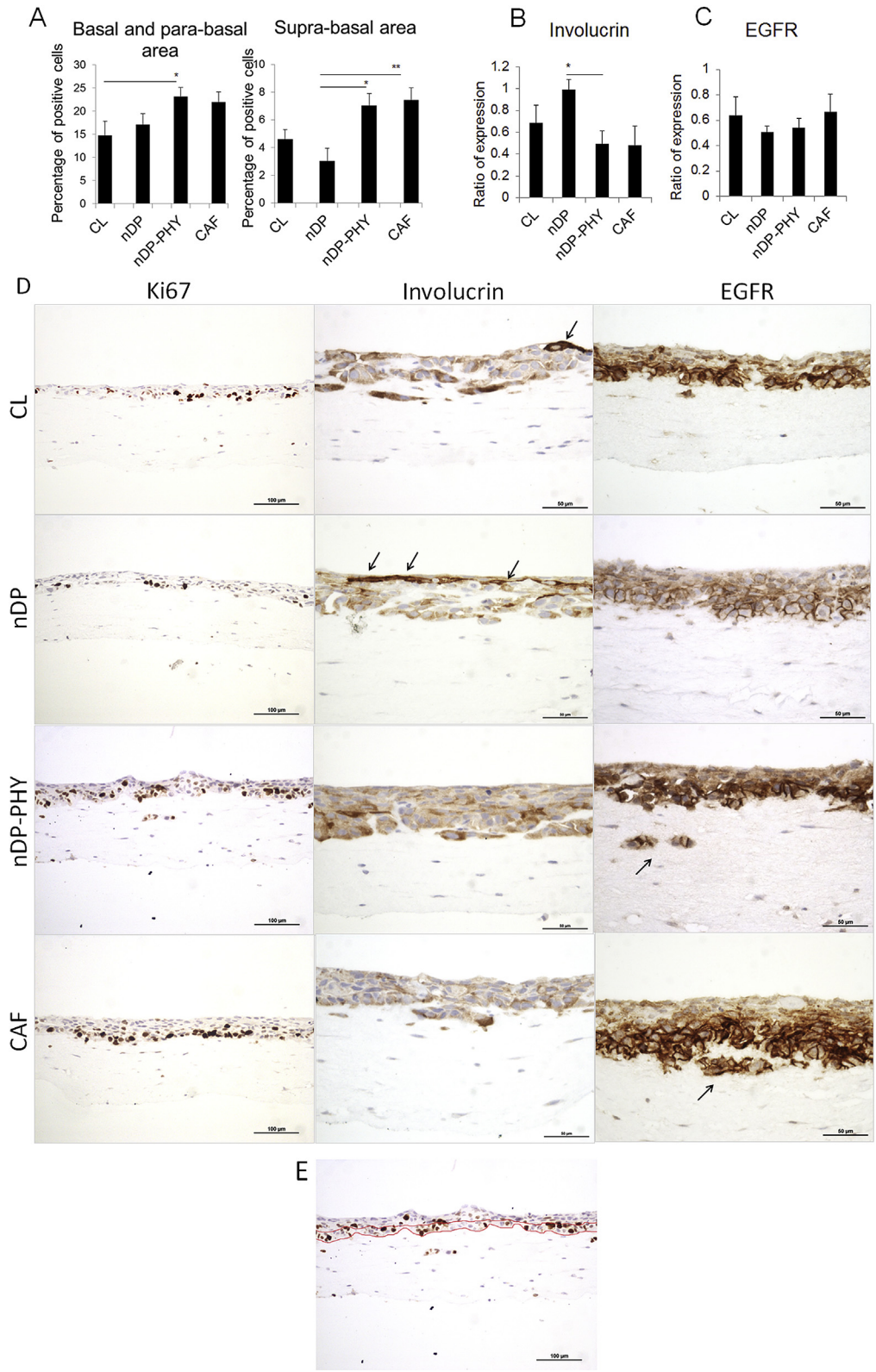

Fig. 2. Proliferating and differentiating capacities of DOK^{Luc} after culture on the different scaffolds. (A) Percentage of Ki67 positively stained nuclei of DOK^{Luc} in the basal and para-basal area and in the supra-basal layers of the epithelial compartment of the 3D-OTs. **(B)** Quantification of involucrin expressed as a ratio of positive cells in supra-basal area to basal and para-basal areas of the epithelial compartment of 3D-OTs formed by DOK^{Luc} previously grown on different scaffolds. **(C)** Quantification of EGFR expressed as a ratio of positive cells in supra-basal area to basal and para-basal areas. **(D)** Representative micrographs of sections stained for Ki67 (Scale bar = 100 μm), involucrin (black arrows point at normal pattern of stain in the superficial layers of the epithelium) and EGFR (black arrows point at invading cells highly expressing EGFR) (Scale bar = 50 μm). All are counterstained with hematoxylin. All immunostains used DAB and the brown colour represents the positive result. Error bars represent SEM. *$p < 0.05$, **$p < 0.01$. **(E)** Descriptive example of how the basal and para basal areas were differentiated. (For interpretation of the references to colour in this figure legend, the reader is referred to the web version of this article.)

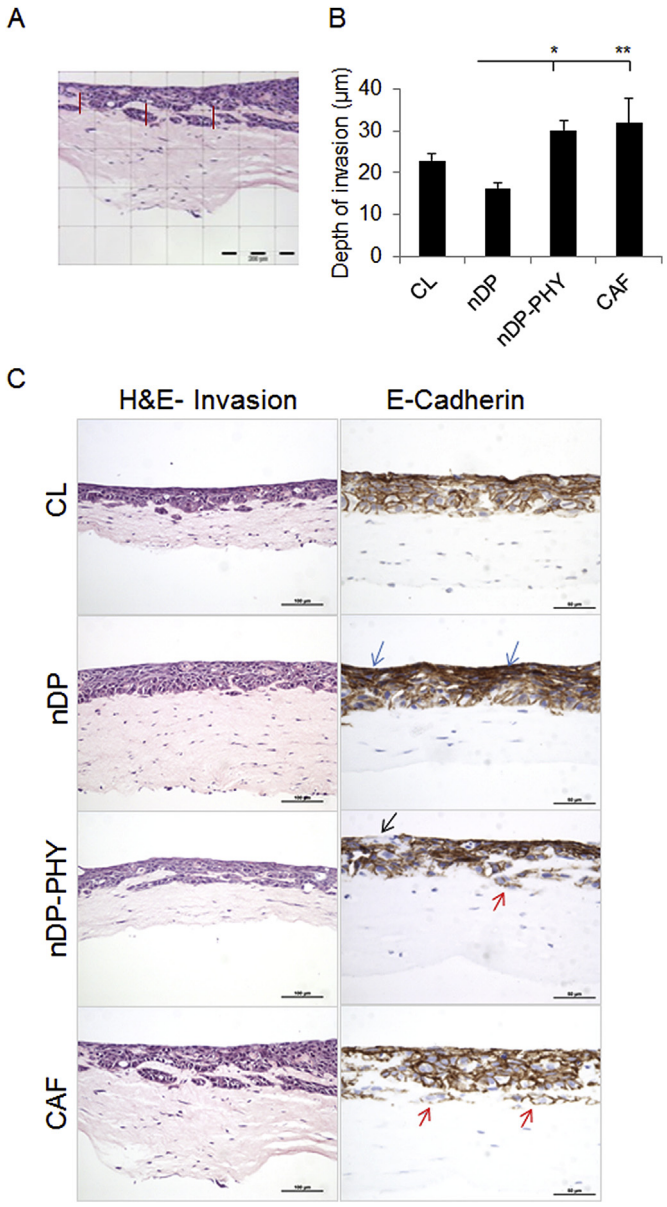

Fig. 3. Invasive potential of DOK^{Luc} after culture on the different scaffolds. (A) Measuring invasion of DOK^{Luc} in the sectioned 3D-OT every 100 μm as the vertical distance from an arbitrary line drawn through the upper remnants of the collagen biomatrix and representing the basement membrane till the deepest limit of invading DOK^{Luc} in the respective field (red lines) **(B)** Quantification of the depth of invasion of the epithelium formed by DOK^{Luc} cells in 3D-OTs. DOK^{Luc} extracted from the different scaffolds were grown on collagen matrices populated with GF. As a positive control for a tumorigenic signal [35] DOK^{Luc} from a monolayer were grown on a matrix populated with CAF. DOK^{Luc} previously grown on nDP scaffolds showed a significantly reduced invasion in the bio-matrix as compared to those from nDP-PHY scaffolds and cells grown on positive control. Error bars represent SEM. $^{*}p < 0.05$, $^{**}<0.01$. **(C)** Left panel displays representative H&E stained sections of 3D-OTs with DOK^{Luc} previously grown on different scaffolds and positive control (CAF) (Scale bar 100 μm). Right panel displays representative E-cadherin stained sections of 3D-OTs with DOK^{Luc} previously grown on different scaffolds and positive control (CAF). Scale bar 50 μm. The immunostaining used DAB and the brown colour represents the positive result. (For interpretation of the references to colour in this figure legend, the reader is referred to the web version of this article.)

the expression was reduced and became more diffuse and less confined to the cell membrane in the parts of the epithelium crossing the basement membrane and invading towards the mesenchymal compartment of the 3D-OT (Fig. 3C, red arrows). Of note, E-cadherin expression was stronger in DOK^{Luc} from nDP scaffolds (Fig. 3C, blue arrows), while showing weaker expression and even negative areas DOK^{Luc} from nDP-PHY scaffolds (Fig. 3C, black arrows).

3.4. DOK^{Luc} cells cultured on nDP scaffolds displayed reduced tumorigenic potential in NSG mice compared to DOK^{Luc} cells cultured on other scaffolds

The total photon intensity of CL scaffolds xenotransplanted with DOK^{Luc} + CAF was significantly higher than of DOK^{Luc} alone throughout the 14 weeks of *in vivo* imaging (Fig. 4). The positive control (DOK^{Luc} + CAF) in the nDP scaffolds also showed higher BLI compared to nDP scaffolds with DOK^{Luc} alone, but up to 8 weeks only. After 8 weeks, the photon counts decreased to values comparable to those of xenografts formed by DOK^{Luc} alone (Fig. 4). On the contrary, the total photon count from nDP-PHY scaffolds carrying DOK^{Luc} + CAF had a significantly higher intensity compared to nDP-PHY scaffolds carrying DOK^{Luc} alone that increased gradually throughout the 14 weeks of imaging. The tumours formed by the scaffolds carrying DOK^{Luc} + CAF were also microscopically examined and the pattern of invasion in the tumour front was classified [43]. Generally, the xenotransplants showed a polarised histological picture with proliferating cells at the periphery and more differentiated areas, including keratin pearls, towards the centre of the scaffold. The nDP-PHY scaffold had the highest number of invasive tumours outside the scaffold area (100%) (Fig. 5B). The pattern of invasion was mostly as small groups or cords of infiltrating cells (>15) (Fig. 5, blue arrows). The lowest number of invasive tumours over the limits of the scaffold area was in the nDP scaffold group with only 2/6 xenografts showing signs of invasion, although the pattern of invasion, when present, was similar to the one seen in nDP-PHY scaffolds (Fig. 5, blue arrows). All xenografts formed by (various scaffolds carrying DOK^{Luc} alone) displayed proliferating DOK^{Luc} well confined to the scaffolds' area. The scaffold was mostly filled with fibrous tissue (Fig. 5, black arrows) and differentiated keratin pearls. When the involucrin stain was carried out in these xenografts, modified scaffolds showed a higher trend of expression compared to CL scaffolds (Fig. 5 C), although not statistically significant.

4. Discussion

This study evaluated the tumorigenic potential of functionalising poly(LLA-co-CL) scaffolds *in vitro*, in addition to using a recently developed *in vivo* non-invasive environmentally-induced oral carcinogenesis model.

Due to the adherent nature of DOK cells, not many cells could be retrieved after typsinization of scaffolds, therefore a propagation period was necessary in order to get enough number of cells to carry out the functional tumorigenicity assays. Measurable differences when using several functional assays after the propagation period could be seen with significant differences between cells grown on the different scaffolds, despite the propagation in culture after the culture on scaffolds.

The DOK^{Luc} previously seeded on nDP scaffolds after being extracted, contained cells with a larger surface area microscopically indicating a more differentiated phenotype for DOK^{Luc} seeded on these scaffolds. This is consistent with previous reports that proposed nanoparticle modification of scaffold material surfaces as an efficient method to increase cell attachment, reducing migration and thus promoting differentiation [28,44]. This seemed to be related to the improvement in topography and nano-scale architecture which resembles closer the extracellular matrix and to the

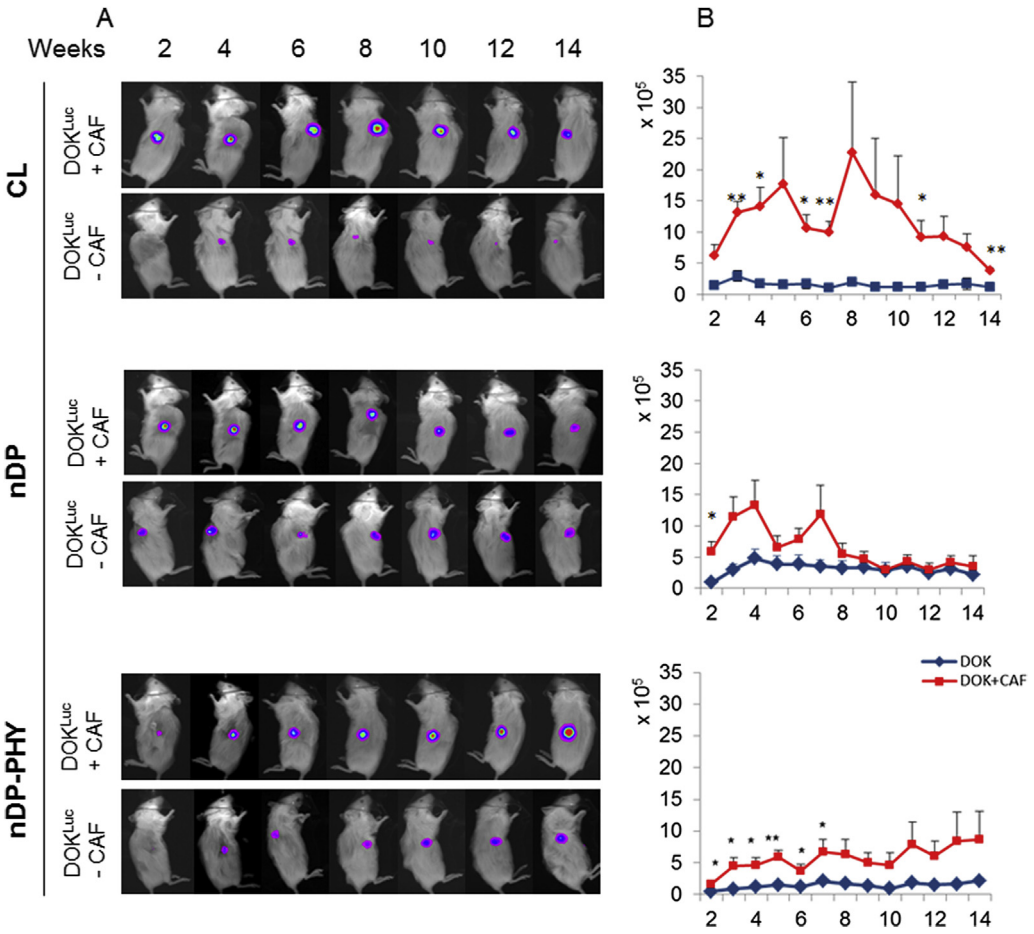

Fig. 4. ***In vivo*** **monitoring of tumour formation. (A)** Bioluminescence images from even weeks where a representative mouse from each scaffold group is displayed. Two scaffolds were implanted into each mouse, one xenotransplanted with DOK^{Luc} alone (negative control) (lower banner) and another with DOK^{Luc} + CAF (positive control) (upper banner) (n = 6). **(B)** Total photon count y axis = (photons × 10^5/mm^2/sec) from *in vivo* imaging of mice carrying different scaffolds xenotransplanted with negative and positive control throughout 14 weeks of imaging. Data presented as mean ± SEM. *p < 0.05, **<0.01.

functional charged terminal groups present in nDP [28]. A recent study using lactate dehydrogenase test on poly (lactic-*co*-glycolic acid) membranes modified with nDP, reported no significant difference in cytotoxicity of mesenchymal stem cells (MSC) for up to 9 days compared to unmodified membranes [44]. Another study on osteoblasts found that the cells exhibited poorer proliferation but significantly improved long-term functions such as differentiation markers when cultured on nanocrystalline diamond surfaces compared to counterpart tested materials due to appropriate nanotopography [45].

The result of the non-adherent culture that showed the highest number of spheres were found to be from DOK^{Luc} previously seeded on nDP-PHY scaffolds is in line with a recent study that proved that BMP-2-treated colon cancer cells formed spheres that displayed significantly elevated expression of stemness markers via STAT3 transcription factor [46].

The DOK^{Luc} previously grown on nDP scaffolds displayed a less abnormal proliferation pattern in 3D-OT models when compared with DOK^{Luc} previously grown on other scaffolds. In a normal oral epithelium, the basal and para-basal layer is the only proliferative compartment, the rest of the epithelial layers display maturation without any proliferative activity. Increased cell proliferation, and particularly the abnormal presence of proliferating cells in the supra-basal layers is a feature of transition to dysplasia and to malignancy [47]. Thus, proliferation observed in supra-basal areas in certain conditions as that significantly seen in nDP-PHY scaffold as well the positive control raises concern on the carcinogenic potential of that particular condition that should be taken with caution. The cells from the nDP and CL scaffolds showed cell proliferation more towards the normal distribution of proliferating cells in oral epithelium, confined to the basal layer. A previous study that used Ki-67 in assessing the severity of epithelial dysplasia demonstrated that the supra-basal expression provides an independent criteria for determining the severity and histological grading of OSCC [48]. These results emphasise the role nanodiamonds might play in suppressing a dysplastic or abnormal epithelial phenotype, thus pinpointing their potential for reducing the tumorigenic risk. In a similar 3D-OT model, a comparable pattern of Ki-67 staining equally distributed throughout all epithelial layers was also noted when neoplastic human oral keratinocytes (PE/CA-PJ 15 cell line) were cultured on top of the collagen with fibroblasts which, based on other parameters as well, were shown to represent a late stage oral carcinogenesis [49]. The high expression of Ki-67 in nDP-PHY can be attributed to the BMP-2, its enhancement effects on proliferation being reported previously, such as in ovarian cancer cells [50]. The reduced proliferation seen in nDP modified scaffold group can be also considered a check point to reduce errors accompanied with proliferation. However, there are reports showing that incubating embryonic stem cells with nanodiamonds led to mild DNA damage, particularly when

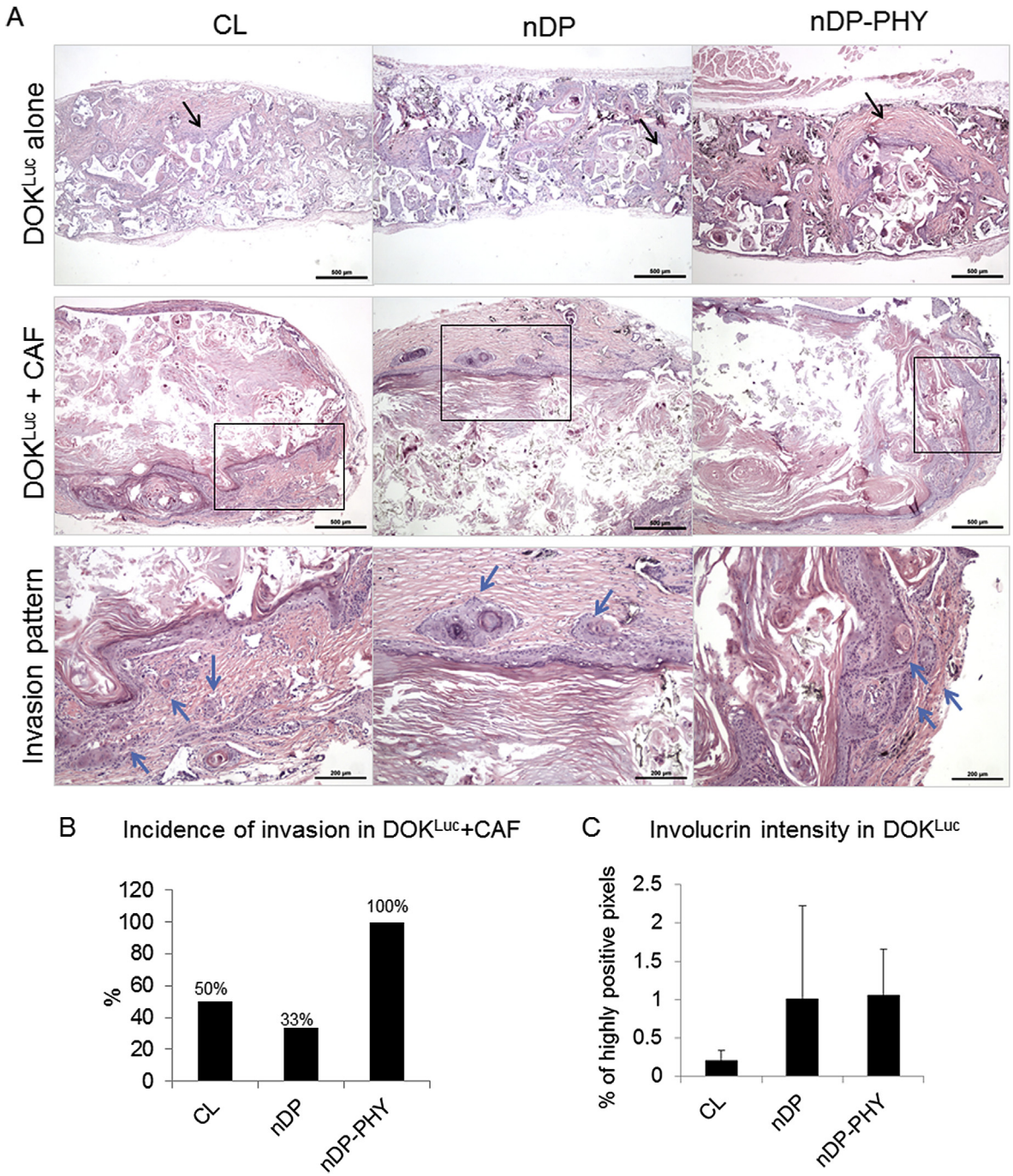

Fig. 5. Histology of the different scaffolds carrying DOK^{Luc} or DOK^{Luc} + CAF after 14 weeks *in vivo*. **(A)** H&E sections showing histology of the different scaffolds carrying DOK^{Luc} or DOK^{Luc} + CAF after 14 weeks *in vivo*. First uppermost panel shows DOK^{Luc} alone, scale bar = 500 μm. Middle panel shows DOK^{Luc} + CAF, scale bar = 500 μm. Lowest panel shows invasion patterns in DOK^{Luc} + CAF, scale bar = 200 μm. **(B)** Incidence of invasion from tumours formed in scaffolds carrying DOK^{Luc} + CAF **(C)** Quantification of the involucrin staining expressed as percentage of highly positive pixels showing higher differentiation trend in the nDP modified scaffolds, although not significant. Error bars represent SEM.

using oxidised nanodiamonds, upregulating the DNA repair proteins. The authors alleged that this damage was much less severe than that caused by carbon nanotubes and it was probably attributed to reactive oxygen species [51]. The enhanced tumorigenic potential in the DOK^{Luc} could be due to BMP-2 or cross talk with excretory molecules from CAF, leading to the reduced differentiation and promoted proliferation as shown in Fig. 2 for those respective conditions. The involucrin results corroborate well with the Ki-67 results, in line with a similar study comparing different scaffolds used to construct organotypics of oral mucosa, which also reported variable degrees and patterns of maturation or stratification in the epithelium as detected by immunohistochemistry, depending on the scaffold used [52]. This demonstrates that the topography of artificial extracellular matrices plays a role in the fate of the cultured cells. Epithelial growth factor receptor (EGFR) is a tyrosine kinase receptor highly expressed in several solid tumours, including oral cancers and is related with increased proliferation, invasion and poor prognosis of OSCC [53,54]. The pattern of EGFR staining observed in our 3D-OT, although not significant, showed an opposite trend to the involucrin stain.

The DOK^{Luc} cells previously grown on nDP scaffolds displayed lower invasive potential in 3D-OT when compared to DOK^{Luc} previously grown on other scaffolds. Tissue invasion is one of the acquired hallmarks of cancer cells [55]. In a recent study evaluating the effect of BMP-2 on the invasive capacity of OSCC cell lines, the authors also used a co-culture model taking advantage of different cells interacting in cancer and demonstrated how invasion could not be evaluated when the cancer cells were in monoculture. This underlines the role of stromal fibroblasts or cancer microenvironment [41,49]. Similar to our findings, rhBMP-2-treated human OSCC cell lines were found to show enhanced invasiveness and this was dependent on the baseline mRNA expression of BMP-2 in these cells [12]. Other cancer cell lines, such as colon cancer were also found to have enhanced migratory and invasive potentials in response to BMP-2 by induced epithelial-mesenchymal transition (EMT) and downregulated E-cadherin [46]. This should not be surprising, since a normal physiological EMT-promoting effect during development and wound repair is known to be played by BMPs [16,56]. A similar morphology of the expanded intercellular spaces along the length of the epithelium to that seen in DOK^{Luc} grown on collagen biomatrices populated with CAF was previously reported in oral mucosa constructs made with an established OSCC cell line (PE/CA-PJ) [49]. This loss of intercellular adherence has been for long considered a characteristic associated to oral epithelial atypia in patient tissue samples [57]. However, the significant decrease in the DOK^{Luc} invasion was observed in the 3D-OTs that were seeded with DOK^{Luc} from nDP scaffold highlights the role played by the nDP in reducing the tumorigenic potential of DOK^{Luc}. DOK^{Luc} cells previously grown on nDP scaffolds displayed increased expression of cell adhesion molecule E-cadherin when compared to DOK^{Luc} previously grown on other scaffolds. This pattern of staining is in accordance to the histomorphometric measurements for quantifying the invasive potential (Fig. 3B).

To date, there are limited reports evaluating the carcinogenicity of nanodiamond particles *in vivo*. The genotoxicity and nuclear activity tests accompanied with oxidative stress reported in some cell lines [58], do not give a fully functional dimension. Our recently developed tumorigenicity *in vivo* model using BLI showed successful application for screening functionalised copolymer scaffolds intended for BTE (Fig. 4A and B). The total photon intensity of CL scaffolds xenotransplanted with DOK^{Luc} + CAF was in line with the recently published report [33]. The reduced intensity observed in the positive control (DOK^{Luc} + CAF) in the nDP modified scaffolds from 8 weeks could be due to the nanodiamond modification of the scaffold that might play a role in differentiating the tumours and reducing their growth. The fact that the xenografts formed by nDP-PHY scaffolds carrying DOK^{Luc} + CAF did not show a reduction in the BLI as observed in the nDP scaffolds can be attributed to the BMP-2 physisorbed onto the scaffolds and it is in accordance to the *in vitro* results of sphere formation and 3D-OT assays. The higher number of invasive tumours observed from the nDP-PHY scaffold group is in line with a previous study in an orthotopic mouse model which showed that xenografts from rhBMP-2-pre-treated OSSC cell lines formed tumours with more rapid growth compared to control and exhibited poorly differentiated morphology with poorer survival rate [11]. The potential role of BMP-2 in malignant transformation and progression of cancer is still poorly understood despite numerous reported studies. Some reports have shown results of BMP-2 with a tumour suppressing effect in sarcomas, which is in contrary to what studies in OSCC have reported. A study done on a canine osteosarcoma model showed that the treatment using the combination of stem cells from canine bone marrow and BMP-2 was beneficial for the host and could emerge as a potential therapeutic tool for osteosarcoma [59]. The effect of BMP-2 might depend on the tumour type, but several other studies have also suggested a tumour suppressor effect from BMP-2 signalling that inhibit proliferation and growth of colorectal cancer cells and osteosarcoma [60,61], so the issue is still a matter of debate. Additionally, the xenografts carrying DOK^{Luc} alone in all groups showed proliferating cells confined to the scaffold area explaining the constant low photon intensities in the negative controls. The nDP modified scaffolds expressed higher trend of involucrin stain, in line with the *in vitro* results.

5. Conclusions

Taken together, the results presented in this study demonstrated that nDP modified copolymer scaffolds decreased the tumorigenic potential of DOK^{Luc} as shown by their reduced invasiveness, promoted differentiation and reduced adherence-independent growth *in vitro*. These nDP modified scaffolds were observed to reduce the size of tumours formed by DOK^{Luc} + CAF *in vivo* as observed by BLI. This effect of nDP on tumorigenicity encourages in-depth studies on the mechanism behind it to support their use in anti-cancer drug delivery after tumour resection. The therapeutic use of BMP-2 should be cautioned in reconstruction of bone defects in oral cancer patients and further investigations on the bipolar effects of BMP-2 on tumorigenesis are warranted.

Acknowledgements

The research leading to these results has received funding by the European Union's Seventh Framework Programme under grant agreement number 242175-VascuBone, Bergen Medical Research Foundation (D.E. Costea, grant no. 20/2009); Helse Vest (D.E. Costea, grant no. 911902/2013); Helse Vest (E.MCormack, grant no. 911884 and 911789). We are grateful to Mrs. Gunnvor Øijordsbakken, Mr. Bendik Nordanger, Mrs. Siren Hammer Østvold and Mrs. Mihaela Popa (Kin*N* Therapeutics) for excellent technical assistance. The bioluminescence imaging was performed at the Molecular Imaging Centre (MIC), University of Bergen.

References

[1] T.N. Vo, F.K. Kasper, A.G. Mikos, Strategies for controlled delivery of growth factors and cells for bone regeneration, Adv. Drug Deliv. Rev. 64 (2012) 1292–1309.
[2] A.H. Reddi, BMPs: from bone morphogenetic proteins to body morphogenetic proteins, Cytokine Growth Factor Rev. 16 (2005) 249–250.
[3] A.S. Herford, P.J. Boyne, Reconstruction of mandibular continuity defects with bone morphogenetic protein-2 (rhBMP-2), J. Oral Maxillofac. Surg. 66 (2008) 616–624.
[4] R.G. Triplett, M. Nevins, R.E. Marx, D.B. Spagnoli, T.W. Oates, P.K. Moy, et al., Pivotal, randomized, parallel evaluation of recombinant human bone morphogenetic protein-2/absorbable collagen sponge and autogenous bone graft for maxillary sinus floor augmentation, J. Oral Maxillofac. Surg. 67 (2009) 1947–1960.
[5] P.J. Boyne, L.C. Lilly, R.E. Marx, P.K. Moy, M. Nevins, D.B. Spagnoli, et al., De novo bone induction by recombinant human bone morphogenetic protein-2 (rhBMP-2) in maxillary sinus floor augmentation, J. Oral Maxillofac. Surg. 63 (2005) 1693–1707.
[6] E.J. Woo, Adverse events reported after the use of recombinant human bone morphogenetic protein 2, J. Oral Maxillofac. Surg. 70 (2012) 765–767.
[7] R.B. Bell, C. Gregoire, Reconstruction of mandibular continuity defects using recombinant human bone morphogenetic protein 2: a note of caution in an atmosphere of exuberance, J. Oral Maxillofac. Surg. 67 (2009) 2673–2678.
[8] E.J. Carragee, E.L. Hurwitz, B.K. Weiner, A critical review of recombinant human bone morphogenetic protein-2 trials in spinal surgery: emerging safety concerns and lessons learned, Spine J. 11 (2011) 471–491.
[9] C.A. Tannoury, H.S. An, Complications with the use of bone morphogenetic protein 2 (BMP-2) in spine surgery, Spine J. 14 (2014) 552–559.
[10] J. Vavken, A. Mameghani, P. Vavken, S. Schaeren, Complications and cancer rates in spine fusion with recombinant human bone morphogenetic protein-2 (rhBMP-2), Eur. Spine J. (2015). Epub ahead of print.
[11] N.A. Kokorina, J.S. Lewis Jr., S.O. Zakharkin, P.H. Krebsbach, B. Nussenbaum, rhBMP-2 has adverse effects on human oral carcinoma cell lines in vivo,

Laryngoscope 122 (2012) 95–102.
[12] N.A. Kokorina, S.O. Zakharkin, P.H. Krebsbach, B. Nussenbaum, Treatment effects of rhBMP-2 on invasiveness of oral carcinoma cell lines, Laryngoscope 121 (2011) 1876–1880.
[13] J.H. Clement, M. Raida, J. Sanger, R. Bicknell, J. Liu, A. Naumann, et al., Bone morphogenetic protein 2 (BMP-2) induces in vitro invasion and in vivo hormone independent growth of breast carcinoma cells, Int. J. Oncol. 27 (2005) 401–407.
[14] J.P. Sand, N.A. Kokorina, S.O. Zakharkin, J.S. Lewis Jr., B. Nussenbaum, BMP-2 expression correlates with local failure in head and neck squamous cell carcinoma. Otolaryngology–head and neck surgery, Off. J. Am. Acad. Otolaryngol. Head Neck Surg. 150 (2014) 245–250.
[15] L. Yang, K. Yamasaki, Y. Shirakata, X. Dai, S. Tokumaru, Y. Yahata, et al., Bone morphogenetic protein-2 modulates Wnt and frizzled expression and enhances the canonical pathway of Wnt signaling in normal keratinocytes, J. Dermatol. Sci. 42 (2006) 111–119.
[16] C.L. Yan, W.A. Grimm, W.L. Garner, L. Qin, T. Travis, N.M. Tan, et al., Epithelial to mesenchymal transition in human skin wound healing is induced by tumor necrosis factor-alpha through bone morphogenic Protein-2, Am. J. Pathol. 176 (2010) 2247–2258.
[17] V.N. Mochalin, O. Shenderova, D. Ho, Y. Gogotsi, The properties and applications of nanodiamonds, Nat. Nanotechnol. 7 (2012) 11–23.
[18] A. Krueger, Beyond the shine: recent progress in applications of nanodiamond, J. Mater. Chem. 21 (2011) 12571.
[19] L. Moore, M. Gatica, H. Kim, E. Osawa, D. Ho, Multi-protein delivery by nanodiamonds promotes bone formation, J. Dent. Res. 92 (2013) 976–981.
[20] A.M. Schrand, H.J. Huang, C. Carlson, J.J. Schlager, E. Osawa, S.M. Hussain, et al., Are diamond nanoparticles cytotoxic? J. Phys. Chem. B 111 (2007) 2–7.
[21] V. Thomas, B.A. Halloran, N. Ambalavanan, S.A. Catledge, Y.K. Vohra, In vitro studies on the effect of particle size on macrophage responses to nanodiamond wear debris, Acta Biomater. 8 (2012) 1939–1947.
[22] H. Tsuda, J.G. Xu, Y. Sakai, M. Futakuchi, K. Fukamachi, Toxicology of engineered nanomaterials - a review of carcinogenic potential, Asian Pac. J. Cancer Prev. 10 (2009) 975–980.
[23] J.C. Middleton, A.J. Tipton, Synthetic biodegradable polymers as orthopedic devices, Biomaterials 21 (2000) 2335–2346.
[24] Y. Xue, S. Danmark, Z. Xing, K. Arvidson, A.C. Albertsson, S. Hellem, et al., Growth and differentiation of bone marrow stromal cells on biodegradable polymer scaffolds: an in vitro study, J. Biomed. Mater. Res. A 95 (2010) 1244–1251.
[25] S.B. Idris, S. Danmark, A. Finne-Wistrand, K. Arvidson, A.C. Albertsson, A.I. Bolstad, et al., Biocompatibility of polyester scaffolds with fibroblasts and osteoblast-like cells for bone tissue engineering, J. Bioact. Compat. Polym. 25 (2010) 567–583.
[26] S. Danmark, A. Finne-Wistrand, M. Wendel, K. Arvidson, A.C. Albertsson, K. Mustafa, Osteogenic differentiation by rat bone marrow stromal cells on customized biodegradable polymer scaffolds, J. Bioact. Compat. Polym. 25 (2010) 207–223.
[27] Y. Sun, A. Finne-Wistrand, T. Waag, Z. Xing, M. Yassin, A. Yamamoto, et al., Reinforced degradable biocomposite by homogenously distributed functionalized nanodiamond particles, Macromol. Mater. Eng. 300 (2015) 436–447.
[28] Z. Xing, T.O. Pedersen, X. Wu, Y. Xue, Y. Sun, A. Finne-Wistrand, et al., Biological effects of functionalizing copolymer scaffolds with nanodiamond particles, Tissue Eng. Part A 19 (2013) 1783–1791.
[29] S. Suliman, Z. Xing, X. Wu, Y. Xue, T.O. Pedersen, Y. Sun, et al., Release and bioactivity of bone morphogenetic protein-2 are affected by scaffold binding techniques in vitro and in vivo, J. Control Release 197 (2015) 148–157.
[30] S. Takanashi, K. Hara, K. Aoki, Y. Usui, M. Shimizu, H. Haniu, et al., Carcinogenicity evaluation for the application of carbon nanotubes as biomaterials in rasH2 mice, Sci. Rep. (2012) 2.
[31] D.F. Williams, Carcinogenicity of implantable materials: experimental and epidemiological evidence, Int. Urogynecol. J. 25 (2014) 577–580.
[32] D.F. Williams, Regulatory biocompatibility requirements for biomaterials used in regenerative medicine, J. Mater. Sci. Mater. Med. (2015) 26.
[33] S. Suliman, H. Parajuli, Y. Sun, A.C. Johannessen, A. Finne-Wistrand, E. McCormack, et al., Establishment of a bioluminescence model for microenvironmentally induced oral carcinogenesis with implications for screening bioengineered scaffolds, Head. Neck (2015). Epub ahead of print.
[34] S.E. Chang, S. Foster, D. Betts, W.E. Marnock, DOK, a cell line established from human dysplastic oral mucosa, shows a partially transformed non-malignant phenotype, Int. J. Cancer J. Int. Cancer 52 (1992) 896–902.
[35] D.E. Costea, A. Hills, A.H. Osman, J. Thurlow, G. Kalna, X. Huang, et al., Identification of two distinct carcinoma-associated fibroblast subtypes with differential tumor-promoting abilities in oral squamous cell carcinoma, Cancer Res. 73 (2013) 3888–3901.
[36] P. Vineis, A. Schatzkin, J.D. Potter, Models of carcinogenesis: an overview, Carcinogenesis 31 (2010) 1703–1709.
[37] K. Odelius, P. Plikk, A.C. Albertsson, Elastomeric hydrolyzable porous scaffolds: copolymers of aliphatic polyesters and a polyether-ester, Biomacromolecules 6 (2005) 2718–2725.
[38] A. Krüger, F. Kataoka, M. Ozawa, T. Fujino, Y. Suzuki, A.E. Aleksenskii, et al., Unusually tight aggregation in detonation nanodiamond: identification and disintegration, Carbon 43 (2005) 1722–1730.
[39] J.B. Lorens, Y. Jang, A.B. Rossi, D.G. Payan, J.M. Bogenberger, Optimization of regulated LTR-mediated expression, Virology 272 (2000) 7–15.
[40] G. Dabija-Wolter, M.R. Cimpan, D.E. Costea, A.C. Johannessen, S. Sornes, E. Neppelberg, et al., Fusobacterium nucleatum enters normal human oral fibroblasts in vitro, J. Periodontol. 80 (2009) 1174–1183.
[41] M.J. Kim, K.M. Kim, J. Kim, K.N. Kim, BMP-2 promotes oral squamous carcinoma cell invasion by inducing CCL5 release, PLoS One 9 (2014) e108170.
[42] F. Varghese, A.B. Bukhari, R. Malhotra, A. De, IHC Profiler: an open source plugin for the quantitative evaluation and automated scoring of immunohistochemistry images of human tissue samples, PLoS One 9 (2014) e96801.
[43] M. Bryne, Is the invasive front of an oral carcinoma the most important area for prognostication? Oral Dis. 4 (1998) 70–77.
[44] M.A. Brady, A. Renzing, T.E.L. Douglas, Q. Liu, S. Wille, M. Parizek, et al., Development of composite poly(lactide-*co*-glycolide)-nanodiamond scaffolds for bone cell growth, J. Nanosci. Nanotechnol. 15 (2015) 1060–1069.
[45] L. Yang, B.W. Sheldon, T.J. Webster, The impact of diamond nanocrystallinity on osteoblast functions, Biomaterials 30 (2009) 3458–3465.
[46] B.R. Kim, S.C. Oh, D.H. Lee, J.L. Kim, S.Y. Lee, M.H. Kang, et al., BMP-2 induces motility and invasiveness by promoting colon cancer stemness through STAT3 activation, Tumour Biol. 36 (2015) 9475–9486.
[47] S.S. Birajdar, M. Radhika, K. Paremala, M. Sudhakara, M. Soumya, M. Gadivan, Expression of Ki-67 in normal oral epithelium, leukoplakic oral epithelium and oral squamous cell carcinoma, J. Oral Maxillofac. Pathol. 18 (2014) 169–176.
[48] N. Dwivedi, S. Chandra, B. Kashyap, V. Raj, A. Agarwal, Suprabasal expression of Ki-67 as a marker for the severity of oral epithelial dysplasia and oral squamous cell carcinoma, Contemp. Clin. Dent. 4 (2013) 7–12.
[49] D.E. Costea, A.C. Johannessen, O.K. Vintermyr, Fibroblast control on epithelial differentiation is gradually lost during in vitro tumor progression, Differentiation 73 (2005) 134–141.
[50] J. Peng, Y. Yoshioka, M. Mandai, N. Matsumura, T. Baba, K. Yamaguchi, et al., The BMP signaling pathway leads to enhanced proliferation in serous ovarian cancer-a potential therapeutic target, Mol. Carcinog. 55 (2015) 335–345.
[51] Y. Xing, W. Xiong, L. Zhu, E. Osawa, S. Hussin, L. Dai, DNA damage in embryonic stem cells caused by nanodiamonds, ACS Nano 5 (2011) 2376–2384.
[52] E. Khan, R.M. Shelton, P.R. Cooper, J. Hamburger, G. Landini, Architectural characterization of organotypic cultures of H400 and primary rat keratinocytes, J. Biomed. Mater. Res. Part A 100A (2012) 3227–3238.
[53] F.A. Ribeiro, J. Noguti, C.T. Oshima, D.A. Ribeiro, Effective targeting of the epidermal growth factor receptor (EGFR) for treating oral cancer: a promising approach, Anticancer Res. 34 (2014) 1547–1552.
[54] Y. Hiraishi, T. Wada, K. Nakatani, K. Negoro, S. Fujita, Immunohistochemical expression of EGFR and p-EGFR in oral squamous cell carcinomas, Pathol. Oncol. Res. 12 (2006) 87–91.
[55] D. Hanahan, R.A. Weinberg, Hallmarks of cancer: the next generation, Cell 144 (2011) 646–674.
[56] K.S. Park, B.M. Gumbiner, Cadherin 6B induces BMP signaling and de-epithelialization during the epithelial mesenchymal transition of the neural crest, Development 137 (2010) 2691–2701.
[57] J.J. Smith CaP, Histological Grading of Oral Epithelial Atypia by the Use of Photographic Standards, 1969. Copenhagen.
[58] J. Mytych, A. Lewinska, A. Bielak-Zmijewska, W. Grabowska, J. Zebrowski, M. Wnuk, Nanodiamond-mediated impairment of nucleolar activity is accompanied by oxidative stress and DNMT2 upregulation in human cervical carcinoma cells, Chem. Biol. Interact. 220 (2014) 51–63.
[59] R. Reg, Modulation of angiogenesis and immune response in canine osteosarcoma by BMP-2 and mesenchymal stem cells, J. Stem Cell Res. Ther. 3 (2013).
[60] L. Wang, P. Park, F. La Marca, K. Than, S. Rahman, C.Y. Lin, Bone formation induced by BMP-2 in human osteosarcoma cells, Int. J. Oncol. 43 (2013) 1095–1102.
[61] Y. Zhang, X. Chen, M. Qiao, B.Q. Zhang, N. Wang, Z. Zhang, et al., Bone morphogenetic protein 2 inhibits the proliferation and growth of human colorectal cancer cells, Oncol. Rep. 32 (2014) 1013–1020.